CrystEngComm

Accepted Manuscript

ROYAL SOCIETY OF CHEMISTRY

www.rsc.org/crystengcomm

Crystallization of Poly(butylene 2,6-naphthalate-co-butylene adipate)s: Regulating Crystal Modification of the Polymorphic Parent Homopolymers and Biodegradation

George Z. Papageorgiou*, Vasilios Tsanaktsis, Dimitrios N. Bikiaris*

Laboratory of Polymer Chemistry and Technology, Department of Chemistry, Aristotle University of Thessaloniki, GR-541 24, Thessaloniki, Macedonia, Greece

Abstract

A series of poly(butylene 2,6-naphthalate-co-butylene adipate)s (PBNAd copolymers) were synthesized by the polycondensation method. ^{1}H-NMR showed that the copolymers were random and naphthalene/adipate ratios are close to the feeding ratios. The copolyesters showed isodimorphic cocrystallization. The degree of crystallinity decreased with increasing the comonomer content. Slight variations in the interplanar spacings were observed, indicating cocrystallization. Intriguing morphologies were observed by using polarized light microscopy (PLM). β-crystals of poly(butylene 2,6-naphthalate) (PBN) and large dendrites were in principle formed especially for the PBNAd 90.9/9.1. Thus, polymorphism of PBN was controlled by copolymerization. The thermodynamic analysis of cocrystallization showed limited incorporation of the minor comonomer in the crystals. The adipate units can easier be incorporated in the PBN crystal, than the bulkier naphthalate units in the poly(butylene adipate) (PBAd) crystal. The enzymatic degradation was retarded with increasing the butylene naphthalate content in the copolymers. PBNAd copolymers with more than 60mol% did not hydrolyze.

Keywords: poly(butylene 2,6-naphthalate-co-butylene adipate)s; random copolymers; crystallization rates; biodegradation.

Introduction

Aliphatic polyesters are synthetic polymers with favorable biodegradation characteristics. Unfortunately, the application field of aliphatic polyesters in industry

and agriculture is greatly limited because of their high cost and poor physical and mechanical properties.[1] It is true that biodegradable polymers with sufficient thermal and mechanical properties are still a challenge. In contrast to aliphatic, aromatic polyesters are materials displaying excellent physical properties. However, they are strongly resistant to hydrolysis, as well as bacterial and fungal attack.[2]

To overcome the drawbacks of aliphatic polyesters and aromatic polyesters copolyesters with aliphatic and aromatic moieties have been synthesized. A variety of random copolymers made of a mixture of terephthalic acid and several aliphatic diacids with different diols has been prepared by melt polycondensation, and their structure and properties have been examined in more or less detail.[3-5] Investigations on the syntheses[6-9] characterization[10, 11] and biodegradation behaviour[12-16] of aliphatic–aromatic copolyesters have been reported.

Nowadays, aliphatic/aromatic copolyester materials have already been commercialized. Ecoflex1 of BASF AG[17] and Eastar Bio1 of Eastman Chemicals Company are statistical copolyesters including 1,4-butanediol, adipic acid, terephthalic acid and modular units, and Biomax™ produced by DuPont which is a copolyester based on poly(ethylene terephthalate) (PET) and other aliphatic monomers.[18] BASF has commercialized the biodegradable polyester, Ecoflex™, which consists of several polyester units, containing 1,4-butanediol, adipic acid and terephthalic acid.[19] Reactive blending of homopolyesters is an alternative for producing aliphatic/aromatic copolyesters.[20]

The field of potential applications of aliphatic/aromatic copolyesters and the corresponding blends or nanocomposites has been expanded.[21] Last years, biodegradable aliphatic/aromatic multiblock copolyesters have gained an increasing interest as candidates in applying for biomedical purposes.[22, 23] Understanding of structure-property relationships with respect to biodegradability is of importance for the tailored design of polymeric materials for specific applications, including packaging but also tissue engineering. The physical properties of random copolymers strongly depend on composition and physical properties of the individual homopolymers. Additionally, if both homopolymers are capable of crystallizing, the corresponding random copolymers are likely to develop crystallinity or not mainly depending on the nature of the comonomeric units, composition, and thermal treatment.[24]

Naphthalate thermoplastic polyesters are engineering materials with enhanced thermal, mechanical and barrier properties.[25, 26] Poly(ethylene 2,6-naphthalate) (PEN) and poly(butylene 2,6-naphthalate) (PBN) are the two representative polyesters of the naphthalate family.[27-28] PBN is characterized by excellent mechanical, thermal, gas barrier and electrical properties, which permit its use as biaxially oriented films, fibres, connectors, switches, coil bobbins, ignition coils fuel sensors, fuel tanks and hoses. It is a linear aromatic polyester which consists of a flexible part, butylene, and a rigid one, naphthalate. PBN crystallizes very easily and consequently it is very difficult to obtain an isotropic glass, i.e. a frozen state of melt, by fast cooling.[29] Its crystal structure and polymorphism are of special importance. The more stable β-crystal modification is formed on crystallization at higher temperatures. Copolymers also prefer this modification. Due to the difficulty to obtain an isotropic glass, several values for the glass-transition temperature have been reported in the literature, ranging from 41 to 82^{o}C.[30]

Poly(butylene adipate) (PBAd) is a biodegradable linear aliphatic polyester. It has high biodegradation rate and high thermal stability[31] and can be used in applications in medicine or as an eco-friendly material. PBAd can crystallize into two kinds of crystalline modifications, namely the α and β-crystal form.[32-33] The polymorphism of PBAd is of fundamental importance, because it is strongly related to the crystallization temperature, crystalline structure, morphology, thermal stability, and biodegradability.[34-35] The α-crystal form appears during crystallization at temperatures above 32^{o}C, it is the thermodynamically stable phase. The β-form appears on crystallization at temperatures below 28^{o}C and can completely transform into the α-form upon heating or annealing at higher temperature.[36-39] Both of the pure polymorphs show the typical Maltese-cross spherulites. The mixture of the two polymorphs is observed on crystallization at temperatures in the range 32^{o}C< T_c < 28 ^{o}C and it is also associated with banded spherulites.[40] It is very important that the two different polymorphs of PBAd also show different enzymatic hydrolysis rates.[41] The enzymatic degradation rate of the α-crystal form is faster than that of the β-modification, despite the fact that the α-crystal is thermodynamically more stable and has larger crystallinity and lamellar size than the β-crystal. In turn, the biodegradation rate of the β-crystal is faster than that of the mixture of the two crystal forms.

Molecular design, synthesis, and characterization of new biodegradable polyesters with enhanced biodegradability and good mechanical properties are the scope of most recent publications.[42-46]

In this work an attempt is made to synthesize new aliphatic/aromatic copolyesters containing soft biodegradable butylene adipate segments and hard butylene naphthalene segments. Both PBN and PBAd have fast crystallization rates so they are always semicrystalline and they also show exceptional polymorphism features. From the study of such a copolymer system conclusions can be extracted about the thermal behavior, cocrystallization of the comonomers and polymorphism in case of random copolymers. Finally, the aim of this study is to examine the interconnection between the solid state characteristics and the biodegradability of the copolymers.

Experimental

Materials

Dimethyl-l 2,6-naphthalate (DMN) was obtained from Amoco Chemicals and Fine Acids (purum 99%). Adipic acid (purum 99 %), 1,4-butanediol (purum 99 %) Tetrabutyl titanate (TBT) catalyst of analytical grade and triphenyl-phosphate (TPP) used as heat stabilizer were purchased from Aldrich. All other materials and solvents used were of analytical grade.

Copolymers synthesis

The polyesters and copolyesters were prepared by the two-stage melt polycondensation method (esterification and polycondensation) in a glass batch reactor. In the first step oligo(butylene 2,6-naphthalate) and oligo(butylene adipate) were prepared.[47]

For the preparation of oligo(butylene 2,6-naphthalate) DMN and 1,4-butanediol (BD) at a molar ratio of diester/BD=1/2.2 and the catalyst TBT charged into the reaction tube of the polyesterification apparatus. The reaction mixture was heated to 180^{o}C for 4 h under an inert atmosphere and stirred at a constant speed (300 rpm) while methanol was distilled off. Then, the temperature was raised to 280^{o}C for further 0.5h in order to remove the excess of BD. For the preparation of oligo(butylene adipate), adipic acid and BD at a molar ratio of diacid/BD=1/1.15 were

charged in the reaction tube and the flask was heated under nitrogen for 4 h at 180°C and stirred at a constant speed (300 rpm), with water removed as the reaction by-product of esterification.

In the second stage of preparation, the polycondensation step, appropriate amounts of each oligoester, according to the desired dicarboxylate ratio in the final polyester, and TPP (0.03 wt% of the final polymer), which prevents side reactions, such as etherification and thermal decomposition, were added in the reaction tube. The flask, under a nitrogen atmosphere, was immersed in a thermostated bath at a temperature of 280°C, for samples with naphthalene content down to 70 mol%, and 250°C for the rest, under continuous stirring (500 rpm). A vacuum (5.0 Pa) was applied slowly over a period of 15 min to avoid excessive foaming and to minimize oligomer sublimation, which is a potential problem during the melt polycondensation. The reaction was carried out for 120 min for all prepared materials. After completion, the polyesters were cooled to room temperature with an ice bath and removed from the flask. The copolymers were used without any purification.

Copolymers characterization

Intrinsic viscosity measurement. Intrinsic viscosity [η] measurements were performed using an Ubbelohde viscometer at 30 °C in a mixture of phenol/1,1,2,2-tetrachloroethane (60/40, w/w). The sample was maintained in the above mixture of solvents at 90°C for some time to achieve a complete solution. The solution was then cooled to room temperature and filtered through a disposable membrane filter made from Teflon.

Nuclear Magnetic Resonance (^{1}H-NMR). ^{1}H-NMR spectra of polyesters were obtained with a Bruker spectrometer operating at a frequency of 400 MHz for protons at room temperature. A mixture of deuterated trifluoroacetic acid (DTFA) and chloroform in a ratio 3/1 w/w (DTFA/$CDCl_3$) was used as solvent in order to prepare solutions of 5% w/v. The number of scans was 10 and the sweep width was 6 kHz.

Wide angle X-Ray diffraction patterns (WAXD). X-ray diffraction measurements of the samples were performed using a MiniFlex II XRD system from Rigaku Co, with CuK_α radiation (λ=0.154 nm) in the angle 2θ range from 5 to 60 degrees.

Differential Scanning Calorimetry (DSC). A Perkin–Elmer, Pyris Diamond DSC differential scanning calorimeter, calibrated with pure Indium and Zinc

standards, was used. The system also included an Intracooler 2P cooling accessory, in order the DSC apparatus to achieve function at sub-ambient temperatures and high cooling rates. Samples of 5±0.1 mg sealed in aluminium pans were used, to test the thermal behavior of the quenched copolymers. The samples were cooled to –70^{o}C and then heated at a rate 20°C/min to above the melting temperature. In order to obtain amorphous materials, the samples were heated to 40 ^{o}C above the melting temperature and held there for 5 min, in order to erase any thermal history, before cooling in the DSC with the highest achievable rate.

Isothermal crystallization experiments of the copolymers at various temperatures below the melting point were performed after self-nucleation of the polyester sample. Self-nucleation measurements were performed in analogy to the procedure described by Fillon et al.[48-50] The protocol used is very similar with that described by Müller et al. [50] and can be summarized as follows: a) melting of the sample at 40 ^{o}C above the observed melting point for 5 min to erase any previous thermal history; b) cooling at 10 ^{o}Cmin^{-1} to a reference temperature and crystallization, to create a ‘‘standard’’ thermal history; c) partial melting by heating at 20 ^{o}Cmin^{-1} up to a ‘‘self-nucleation temperature’’, T_s which differed for the various polymers ; d) thermal conditioning at T_s for 5 min. Depending on T_s, the crystalline polyester will be completely molten, only self-nucleated or self-nucleated and annealed. If T_s is sufficiently high, no self-nuclei or crystal fragments can remain (T_s Domain I - complete melting domain). At intermediate T_s values, the sample is almost completely molten, but some small crystal fragments or crystal memory effects remain, which can act as self-nuclei during a subsequent cooling from T_s, (T_s Domain II-self - nucleation domain). Finally, if T_s is too low, the crystals will only be partially molten, and the remaining crystals will undergo annealing during the 5 min at T_s, while the molten crystals will be self-nucleated during the later cooling, (T_s Domain III - self-nucleation and annealing domain); e) cooling scan from T_s at 200 ^{o}Cmin^{-1} to the crystallization temperature (T_c), where the effects of the previous thermal treatment will be reflected on isothermal crystallization; f) heating scan at 20 ^{o}Cmin^{-1} to 300^{o}C, where the effects of the thermal history will be apparent on the melting signal. Experiments were performed to check that the sample did not crystallize during the cooling to T_c and that a full crystallization exothermic peak was recorded

at T_c. In heating scans after isothermal crystallization the standard heating rate was 20°C/min.

To investigate the non-isothermal crystallization behaviour of the fast crystallizing copolymers, the same melting procedure as described above for the isothermal crystallization was followed and then the samples were cooled from the melt at different cooling rates ranging from 2.5 to 20°C/min.

Polarizing Light microscopy (PLM). A polarizing light microscope (Nikon, Optiphot-2) equipped with a Linkam THMS 600 heating stage, a Linkam TP 91 control unit and also a Jenoptic ProgRes C10Plus camera with the Capture Pro 2.1 software was used for PLM observations.

Enzymatic hydrolysis. Polyesters in the form of films 5x5 cm in size and approximately 0.4 mm thickness, prepared by melt-pressing using a hydraulic press, were placed in petries containing phosphate buffer solution (pH 7.2) with 0.09 mg/mL *Rhizopus delemar* lipase and 0.01 mg/mL of *Pseudomonas Cepacia* lipase. The petries were then incubated at 37±1°C in an oven for several days while the media was replaced every 3 days. After a specific period of incubation (every 72 hours), the films were removed from the petri, washed with distilled water, dried in a vacuum oven at 35°C and weighted until constant weight. The degree of enzymatic hydrolysis was estimated from the mass loss.

Scanning Electron microscopy (SEM). The morphology of the prepared films before and after enzymatic hydrolysis was examined in a scanning electron microscopy system (SEM) type Jeol (JMS–840) equipped with an energy-dispersive X-ray (EDX) Oxford ISIS 300 micro-analytical system. The films were covered with a carbon coating in order to have good conductivity of the electron beam. Operating conditions were: accelerating voltage 20KV, probe current 45 nA and counting time 60 seconds.

Results and Discussion

Synthesis and Molecular Characterization of the PBNAd Copolymers

PBNAd copolymers were synthesized following the two-step melt polycondensation method. First butylene-2,6-naphthalate and butylene adipate oligomers were prepared. Proper amounts of the two species of oligomers were then mixed and polycondensation followed to arrive to copolymers. The use of proper amounts of

oligomers assures that the composition of the copolymers will be close to the scheduled one, as only diol or water molecules, are removed during polycondensation and thus the content in naphthalene and adipate segments remains practically the same as in the mixture of oligomers. Random chain scission due to ester bond cleavage and formation of new ester bonds occurs during this stage at elevated polycondensation reaction temperatures. The chemical structure of the copolymers is shown in Fig. 1.

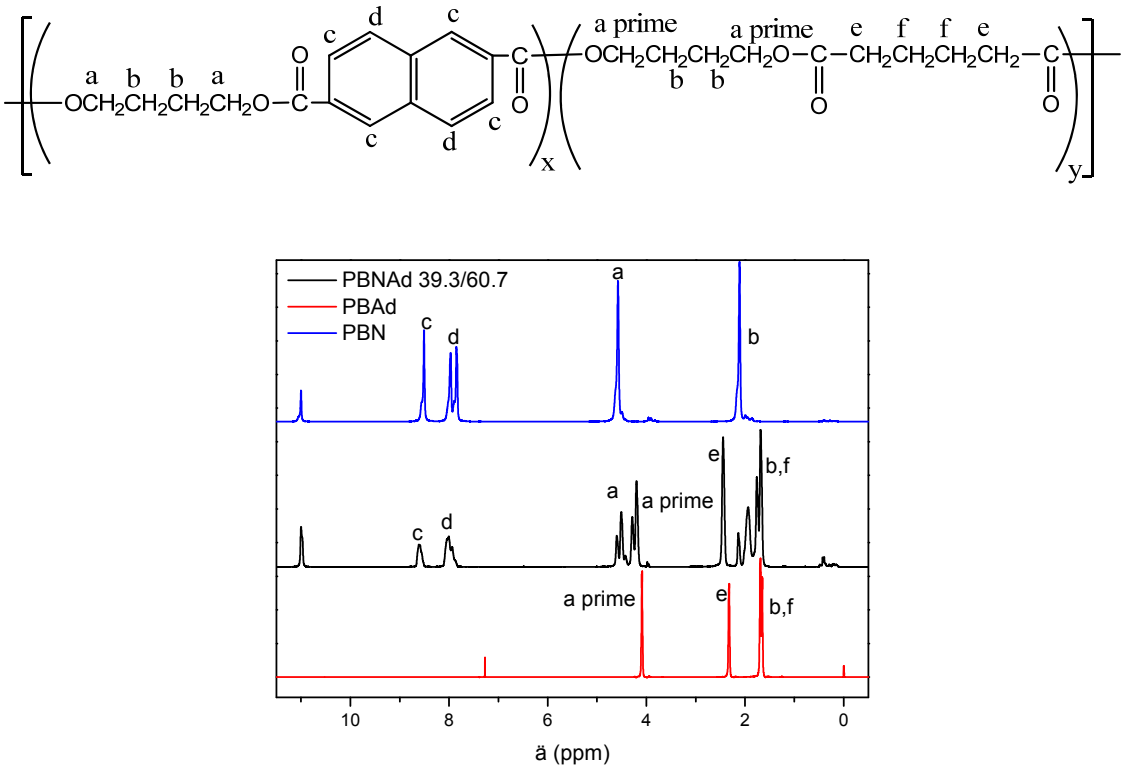

Fig. 1 Chemical structure of poly(butylene naphtalate-co-butylene adipate)s and ^{1}H-NMR spectra of the 39.3/60.7 copolymer and the parent homopolymers.

^{1}H-NMR spectra were collected and used for the determination of copolymer composition as well as for the calculation of the degree of randomness. The spectra were consistent with the expected structures. The ^{1}H-NMR spectrum of poly(butylene naphtalate-co-butylene adipate) 39.3/60.7 mol/mol, together with the corresponding chemical shift assignments, is presented in Fig. 1. For the determination of the copolymer composition the relative peak areas of the c aromatic protons of the naphthalate units (N) located at the region close to 8.8 ppm and the e protons of the methylene groups of the adipic units (Ad) at 2.2 ppm were used. The calculated molar

composition of the copolymers as one see in Table 1 was in all cases close to that in the oligomers' mixture used as feed in the reactor in the step of polycondensation.
The common a protons of the methylene groups appear at 4-4.5 ppm, while the b and f protons of the methylene groups are located at the 1.8-2 ppm area. Finally, the aromatic d protons of the naphthalene groups are located close to the c aromatic protons at 8 ppm. As for the a prime and a protons, they are located at 4.1 and 4.6 ppm respectively. The reason of its splitting is that the a protons are closer to the aromatic bead which deprotects them even more, in addition to the a prime protons which are deprotected mostly by the carbonyl groups. As a result, the a protons appear at higher value.

The degree of randomness (*R*) in the PBNAd copolyesters was calculated using the resonance peaks of the propylene units' aliphatic protons (*a*). The degree of randomness is defined as:[51, 52]

$$R = P_{\mathrm{NAd}} + P_{\mathrm{AdN}} \tag{1}$$

$$P_{\mathrm{TAd}} = \frac{\frac{(f_{NAd} + f_{AdN})}{2}}{\frac{(f_{NAd} + f_{AdN})}{2} + f_{NN}} = \frac{1}{L_{nN}} \tag{2}$$

$$P_{\mathrm{AdT}} = \frac{\frac{(f_{NAd} + f_{AdN})}{2}}{\frac{(f_{NAd} + f_{AdN})}{2} + f_{AdAd}} = \frac{1}{L_{nAd}} \tag{3}$$

where P_{NAd} and P_{AdN} are the probability of finding a Naphthalate (T) unit next to an Adipate (Ad) unit and the probability of finding an Adipate unit next to a Naphthalate unit, respectively. Also f_{NN}, f_{NAd}, f_{AdN}, f_{AdAd} represent the dyads fraction, calculated from the integral intensities of the resonance signals NN, NAd, AdN and AdAd, correspondingly. [47] L_{nAd} and L_{nN} stand for the number average sequence length, the so-called block length, of the Ad and N units, respectively. For random copolymers the degree of randomness R should be equal to 1, while for alternate copolymers equal to 2 and for block copolymers close to zero. Table 1 shows the calculated values for the degree of randomness. Practically these were equal to 1, indicating the PBNAd copolymers of this work were essentially random.

Table 1 Composition, probability of appearance of an adipate unit next to terephthalate (P_{AdT}) and the opposite (P_{TAd}), degree of randomness (R), average block length for adipate (L_{nAd}) and terephthalate (L_{nT}) blocks.

Sample	BN/BAd Feed (mol/mol)	BN/BAd (^{1}HNMR) (mol/mol)	IV (dL/g)	R	L_{nN}	L_{nAd}
PBN	100/0	100/0	0.61	-	-	-
95/5	95/5	90.9/9.1	0.57	0.87	4.09	1.58
90/10	88/12	85.8/14.2	0.63	0.90	3.58	1.58
85/15	82/18	75/25	0.56	0.89	3.57	1.63
70/30	65/35	61.5/38.5	0.60	1.03	2.54	1.54
50/50	45/55	39.3/60.7	0.53	1.00	2.61	1.59
40/60	35/65	37.5/62.5	0.51	0.97	2.27	1.88
20/80	15/85	11.2/88.8	0.61	1.05	1.52	2.43
10/90	8/92	7.1/92.9	0.69	1.06	1.49	2.56
PBAd	0/100	0/100	0.70	-	-	-

The number average sequence length or block length for Napthalate (L_{nN}) and adipate (L_{nAd}) units was calculated using equations 2 and 3, respectively, according to Yamadera and Murano.[53] The corresponding values are also included in Table 1 and it can be seen that by increasing the PBN ratio in copolymers their block length is also increased and the same appears for BAd blocks when the PBAd ratio was higher. However, this variation has no effect on molecular weight of prepared copolymers since all have similar intrinsic viscosity values (Table 1).

DSC Study

The thermal behavior of the copolyesters was investigated using DSC. Fig. 2a shows the DSC heating scans of the as received samples after slow cooling of the reaction tube in air and storage for 1 month at room temperature. All of the polyesters and copolyesters were semicrystalline, although the degree of crystallinity varied. In fact the copolyesters showed lower heat of fusion values with increasing comonomer content reflecting to lower degree of crystallinity. The melting points (T_m) decreased with increasing comonomer unit content and a eutectic behavior was observed i.e. minimum in the plot of T_m with composition. The copolymers with high comonomer content showed wide melting peaks, which indicate a wide distribution of crystal size and degree of crystal perfection. Fig. 2b shows the DSC traces of the quenched samples. As can be seen the copolymers with butylene naphthalate as the major component can crystallize very fast, so only those with more than 25 mol% Adipate

can be obtained in the amorphous state. On the other hand although PBAd crystallizes fast its copolymers with more than 12 mol% Naphthalate content can be efficiently quenched and got amorphous. In these samples cold-crystallization follows the glass transition. Finally, Fig. 2c shows the cooling scans for the copolymers from the melt. In this figure it is obvious that only the copolymers with about 38.5το 88.8 mol% butylene adipate did not crystallize during the cooling scan. The crystallization temperature decreased with increasing the comonomer content showing the difficulty imposed in crystallization due to the shortening of the monomer sequences. Actually, sharp crystallization exotherms appeared on cooling for the homopolymers and the copolymers with low comonomer content. In contrast broad exothermic peaks or complete absence of crystallization were observed for large comonomer content. The transition temperatures and the latent heat values are summarized in Table 2.

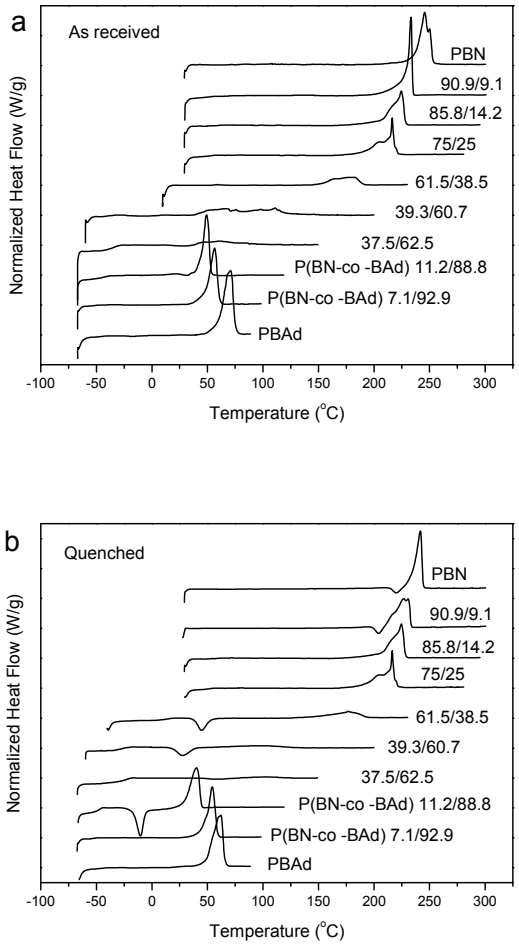

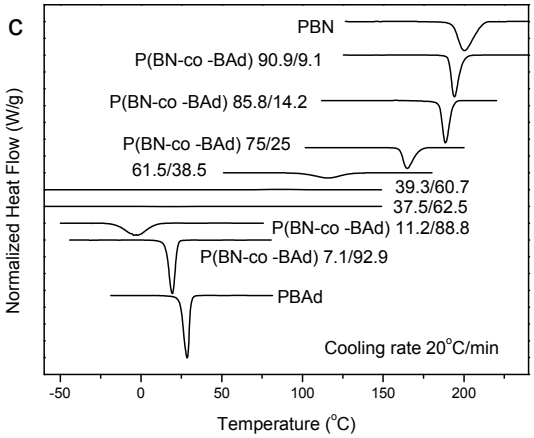

Fig. 2 a) DSC heating scans of crystallized poly(butylene naphthalate-co-butylene adipate)s samples and b) DSC heating scans of the quenched samples. c) DSC cooling scans. Heating or cooling rate 20°C/min.

The observed melting peak temperatures as well as the temperatures at the end of melting are plotted in Fig. 3 as a function of the butylene adipate content. A minimum in the melting point is observed for 88.8 mol% adipate content. The glass transition temperature values show a continuous decrease. As a matter of fact the T_g values for the homopolymers and copolymers with small comonomer content correspond not to amorphous but to semicrystalline samples as these materials crystallize rapidly. The crystallization temperatures on cooling show a trend similar to that of the melting points, meaning a minimum for large comonomer content. However, the difference between the melting and crystallization temperature, that is the supercooling ($\Delta T = T_m - T_c$), increases with increasing comonomer content. Supercooling is the driving force for crystallization, so the large supercoolings needed, verify that crystallization becomes difficult and slower with increasing comonomer content.

Table 2 Transition temperatures and heats of melting crystallization and cold-crystallization for the PBNAd copolymers.

Sample	**BN/BAd** (^{1}HNMR) (mol/mol)	T_m (^oC)	$T_{m\ end}$ (^oC)	T_g (^oC)	T_c (^oC)	T_{cc} (^oC)	ΔH_m (J/g)	ΔH_c (J/g)	ΔH_{cc} (J/g)
PBN	100/0	245.2	255.3	72	200	-	51.3	-41.1	-
95/5	90.9/9.1	233.1	239.0	67	194	-	47.1	-44.3	-
90/10	85.8/14.2	225.5	231.1	60	187	-	38.4	-40.4	-
85/15	75/25	216.4	224.3	52	166	-	29.9	-29.3	-
70/30	61.5/38.5	182.3	193.0	14,5	116	45	19.9	-20.6	-11.7
50/50	39.3/60.7	116.6	124.2	-27	29	26	12.5	-	-12.6
40/60	37.5/62.5	86	93	-31	20	59.7	3.9	-	-3.8
20/80	11.2/88.8	49.1	57.7	-49	-2,5	-10	38.4	-37.8	-30.7
10/90	7.1/92.9	56.7	65.4	-53	19	-	44.6	-48.0	-
PBAd	0/100	68.1	78.3	-60	28,5	-	68.7	51.9	-

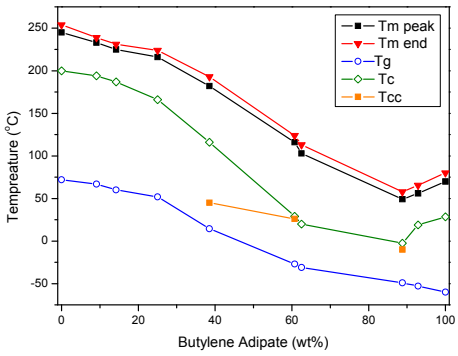

Fig. 3 Melting point ($T_{m\ peak}$), ultimate melting point ($T_{m\ end}$), glass transition temperature (T_g), crystallization temperature on cooling at 20^{o}C/min (T_c), cold crystallization temperature (T_{cc}) as function of the Butylene Adipate content.

The overall isothermal crystallization rates of the PBN homopolymer and the copolymers with up 25 mol% butylene adipate are plotted as a function of the temperature in Fig. 4a. The overall crystallization rates are calculated as the inverse of the crystallization half-time values. The incorporation of the comonomer butylene

adipate units imposes a retardation in crystallization, which is more profound with increasing comonomer content. Fig. 4b shows the crystallization rates of PBAd and the copolymers with up 11.2 mol% butylene adipate. Also, introduction of the comonomer units in the PBAd macromolecular chains cause reduction of the crystallization rates.

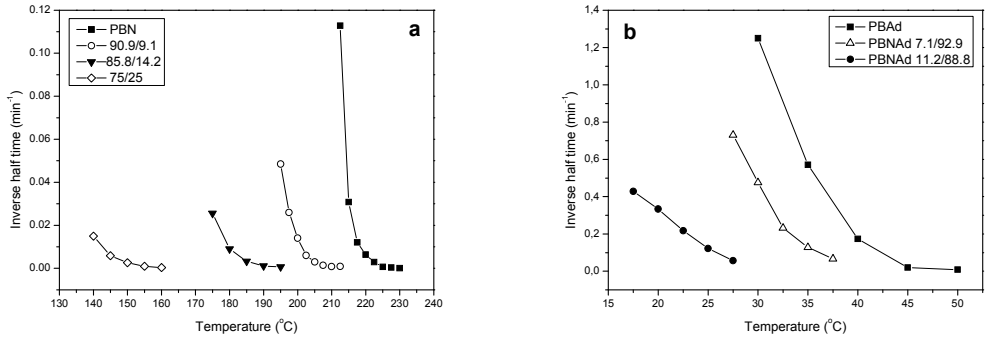

Figure 4. Isothermal crystallization rates for a) PBN and the copolymers with high naphthalate content and b) PBAd and the copolymers with high adipate content.

The melting behavior of the copolymers after isothermal crystallization was also studied in order to better understand the solidification processes and investigate the obtained morphologies. Fig. 5 shows the DSC melting traces for the PBNAd 90.9/9.1, 75/25, 61.5/38.5 and finally the 11.2/88.8 copolymers. For PBNAd 90.9/9.1, 75/25 a multiple melting behavior is obvious. Up to three melting peaks appear in these traces. This behavior verifies that due to the fast crystallization especially under large supercoolings (low crystallization temperatures) metastable crystalline structures are formed, so that, on subsequent heating scans continuous crystal perfection processes involving partial melting and recrystallization occur. For the samples crystallized at low T_cs the peak appearing at the highest temperature has large heat of fusion, in contrast to what is observed in the traces after crystallization at higher T_cs. This is consistent with recrystallization. The sample crystallized at low T_c starts melting at also low temperature. So, during the heating scan there is enough time for recrystallization of the molten material before reaching the final melting temperature and thus the sample recrystallizes significantly giving rise to a large final melting peak. Also, the peak temperature is about stable with increasing the T_c. So, the highest temperature peak is not associated with melting of primary crystals, but it is due to melting of crystals that were subjected to perfection during the heating scan.

It seems that crystal perfection mechanisms do not hold for the PBNAd 61.5/38.5 copolymer, probably because of the slower recrystallization and also because in this sample the adipate content is very large. This means that crystal perfection via abortion of the minor comonomer sequences from the crystal to the amorphous phase is not allowed.[54] Incorporation of the minor comonomer sequences in the crystals results in formation of crystal defects. Also, lamellar thickening is also restricted, as the butylene naphthalate block length, L_{nN}, is drastically reduced to 2.54 compared to 3.57 for the PBNAd 75/25.

The behavior of PBNAd 11.2/88.8 is similar to that of PBAd, (traces for PBAd are not presented here for brevity). Double melting peaks, are observed for this sample.

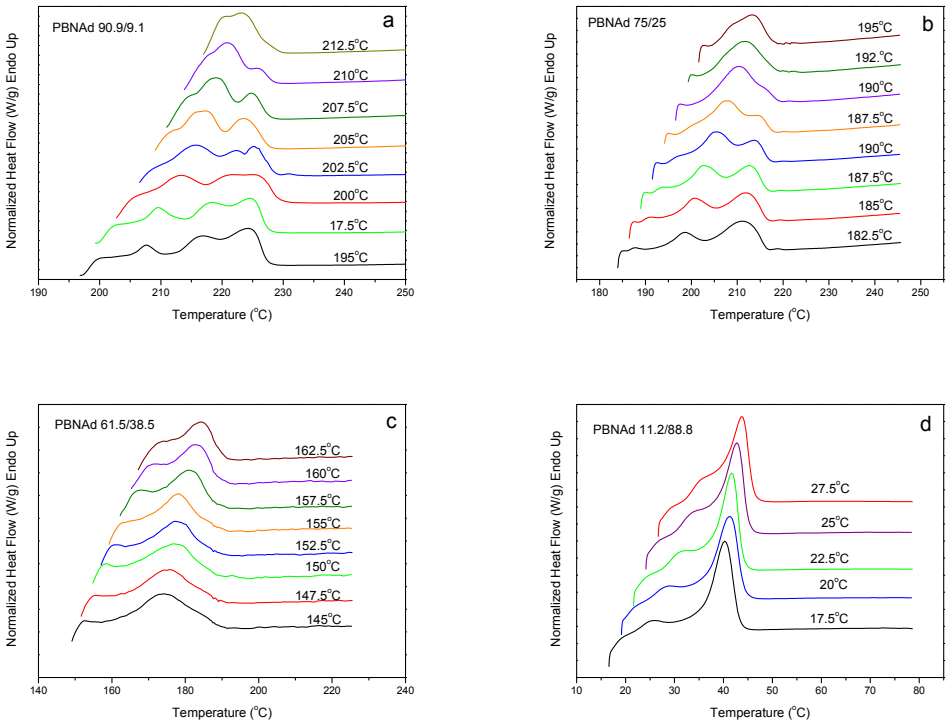

Fig. 5 DSC traces for isothermally crystallized samples at the indicated temperatures: a) PBNAd 90.9/9.1, b) PBNAd 75/25, c) PBNAd 61.5/38.5and c) PBNAd 11.2/88.8.

WAXD Study

Prior to study the crystal structure of the copolymers the crystal structures of the parent homopolymers should be well known. PBN shows two different crystal forms, namely α and β, both in the triclinic crystal system.[31] As was reported in the introduction, PBAd can also crystallize in two forms.[55, 56] The α-crystal form belongs

to the monoclinic, while the β crystal form in the orthorhombic system. The crystal unit parameters of PBN and PBAd are summarized in Table 3. Table 4 correlates the lattice planes with the interplanar spacing and the peak intensities observed in WAXD patterns for PBN. Table 5 shows the corresponding characteristics for PBAd.

Table 3 Crystal structure parameters for PBN and PBAd.

	PBN		PBAd	
Crystal form	α	β	α	β
Crystal system	triclinic	triclinic	monoclinic	orthorhombic
a (nm)	0.487	0.455	0.673	0.506
b (nm)	0.622	0.643	0.794	0.735
c (nm)	1.436	1.531	1.420	1.467
α (deg)	100.78	110.10	90	90
β (deg)	121.10	126.90	45.5^{o}	90
γ (deg)	97.93	100.60	90	90

Table 4 Lattice planes, interplanar spacing and relative intensities corresponding to the peaks appearing in WAXD patterns for PBN.

PBN α- crystal form			PBN β-crystal form		
Lattice plane	Interplanar spacing *d* (nm)	Intensity	Lattice plane	Interplanar spacing *d* (nm)	Intensity
$(0\bar{1}1)$	0.603	M	$(0\bar{1}1)$	0.631	S
(010)	0.579	M	(010)	0.539	S
(011)	0.450	MW	$(\bar{1}03)$	0.416	W
$(\bar{1}11)$	0.406	MW	$(1\bar{1}0)$	0.381	M
(100)	0.369	S	(003)	0.373	W
$(1\bar{1}0)$	0.369	S	(100)	0.348	S
$(1\bar{1}1)$	0.311	MW	$(1\bar{1}1)$	0.330	W

Table 5 Lattice planes, interplanar spacing and relative intensities corresponding to the peaks appearing in WAXD patterns for PBAd.

PBA (α-crystal form)			PBA (β-crystal form)		
Lattice plane	Interplanar spacing *d* (nm)	Intensity	Lattice plane	Interplanar spacing *d* (nm)	Intensity
(110)	0.411	S	(110)	0.416	S
(020)	0.397	S	(020)	0.367	S
(021)	0.306	M	(021)	0.297	M
(200)	0.240	W	(200)	0.253	W

For the study the crystal structure of the copolymers WAXD patterns of the crystallized materials were recorded. In Fig. 6a the WAXD pattern of PBN is shown.

The peaks correspond to reflections of both α and β type crystals. Fig. 6b shows the obtained WAXD pattern for PBAd. In this pattern both α and β crystal type reflections can be seen. The patterns for the copolymers in comparison to the neat homopolymers are shown in Fig. 7a. As can be seen the copolymers show mainly the PBN β crystal type reflections. The PBAd structure was followed by only the PBNAd 7.1/92.9 and 11.2/88.8. Interestingly, the lower melting point was also found for the PBNAd 11.2/88.8 copolymer. It seems that the transition from PBN to PBAd- like crystal structure occurs at this composition or maybe in the range between the PBNAd 37.5/62.5 and 11.2/88.8. However, for the PBNAd 39.3/60.7 and 37.5/62.5 an intermediate structure is observed. The variation of the interplanar spacing *d* for the various lattice plains with composition can be seen in Fig. 7b. A slight decrease in the b and c axis length of the PBN unit cell can be concluded with increasing the butylene adipate content in the copolymers, while the a-axis length seems to increase. This shows the effect of the copolymerization and the introduction of the comonomer adipate units in the PBN-type crystals. A decrease in the cell dimensions would be expected given that butylene naphthalate is a bulkier comonomer than butylenes adipate.

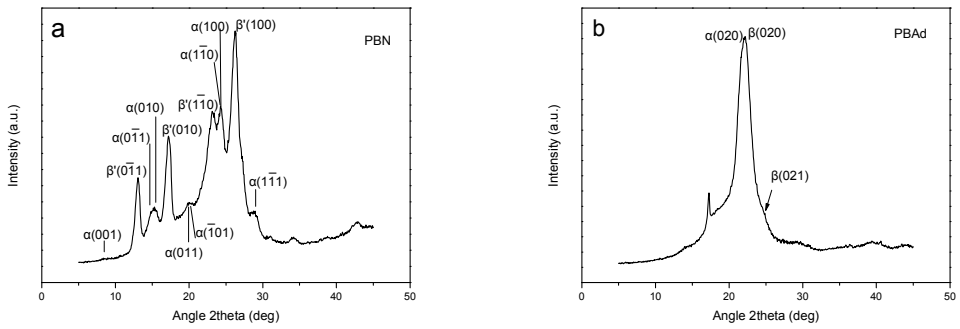

Fig. 6 WAXD patterns for a) PBN and b) PBAd.

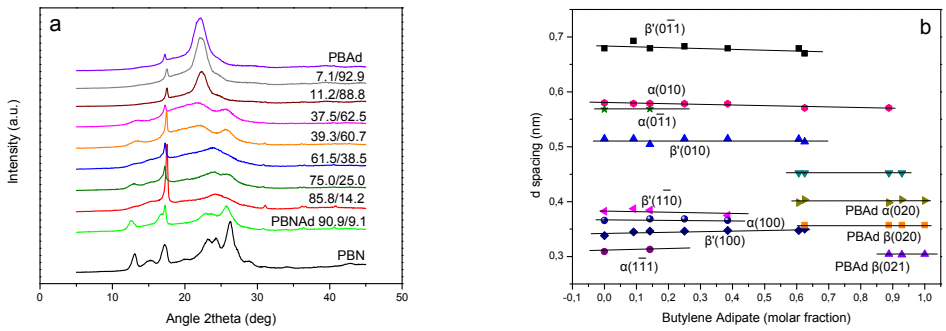

Fig. 7 a) WAXD patterns of the PBNAd copolymers compared to PBN and PBAd and b) variation of the interplanar distances with composition for the PBNAd copolymers.

Polarized Optical Microscopy

POM offers the opportunity to watch directly the formation of a crystalline phase when the sample is cooled from the melt. Fig. 8-10 show a series of POM photographs. Photos of PBAd, PBNAd 7.1/92.9 and 11.2/88.8, 61.5/38.5 and 75/25 are shown in Fig. 8. As PBAd crystallized at 38^{o}C that is above 31^{o}C α-crystals were expected to form. The ringless spherulites observed are indeed associated with the α-crystals of PBAd. The spherulites of PBNAd 7.1/92.9 were smaller. The same was observed for PBNAd 11.2/88.8. This spherulite size reduction, as well as the slower crystallization of the two copolymers compared to PBAd at the same temperatures, are obvious effects of the introduction of the comonomer units in the macromolecular chains. Fig. 8d and e show the structures obtained by the PBNAd 61.5/38.5 during isothermal crystallization at 160 and 165^{o}C respectively. This copolymer shows some trend to form morphologies that deviate from the spherulitic ones at high crystallization temperatures, maybe because not only α, but also β-crystals are formed. The 75/25 copolymer showed also an intriguing morphology that is different from the classic spherulitic.

The case of the PBNAd 90.9/9.1 is of special interest. Fig. 9 shows the morphology obtained after isothermal crystallization at different conditions. As was also concluded from the WAXD patterns, the particular copolymer crystallized preferentially giving β-PBN crystals. Photos of Fig. 9 show dendritic morphologies. Such morphologies are strongly related to the β-crystals.

Finally, in Fig. 10 one can see the photographs of PBN morphologies. At 225^{o}C or lower it seems that spherulitic structures are formed. In Fig. 10c heating at temperatures close to final melting revealed the spherulitic morphology generated at 225^{o}C. As the crystallization temperature increased to 230^{o}C or higher dendrites became more obvious and dominated. This observation indicates that α crystals are formed at lower temperatures while β crystals and the corresponding dendritic morphologies are formed at higher temperatures.

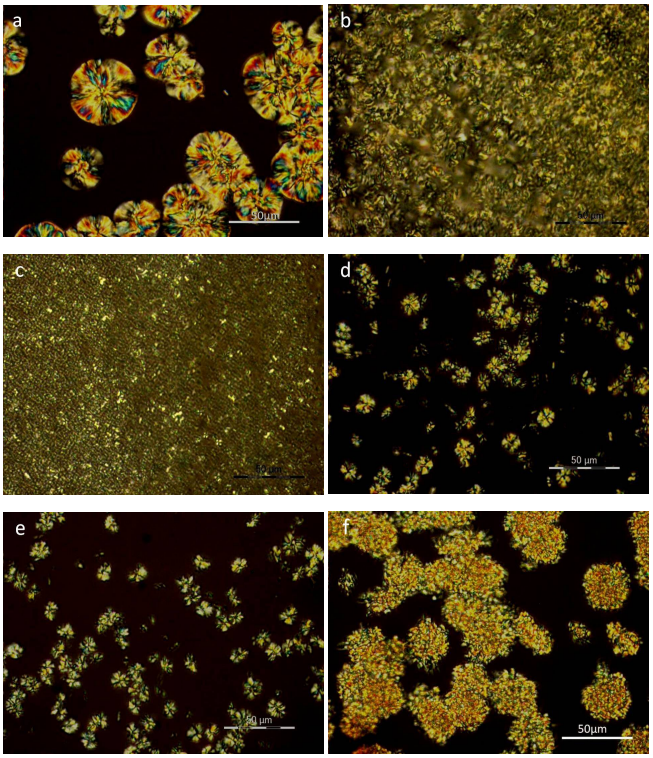

Fig. 8 POM photographs shown morphologies for: a) PBAd crystallized from the melt at 38°C, b) PBNAd 7.1/92.9 at 35°C, c) PBNAd 11.2/88.8 at 28°C, d) PBNAd 61.5/38.5 at 160°C, e) PBNAd 61.5/38.5 165°C and f) PBNAd 75/25 at 195°C.

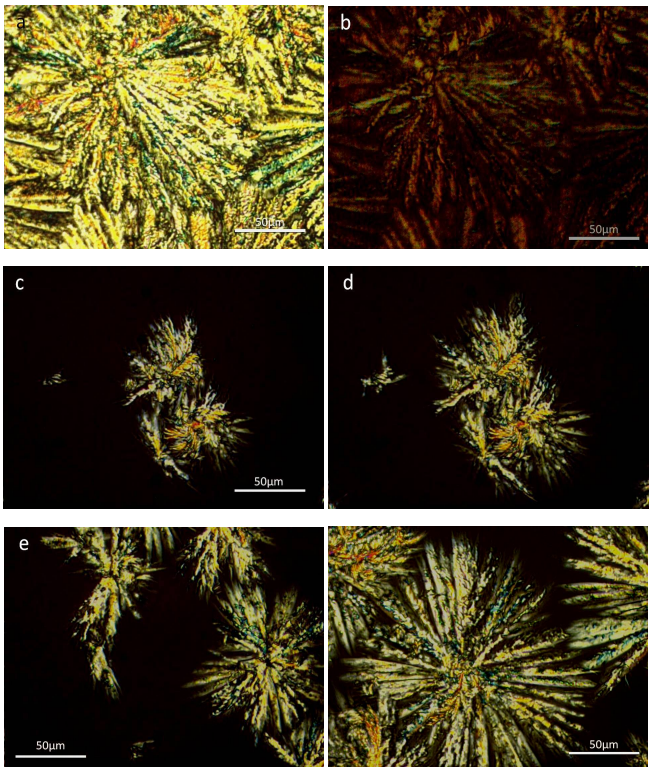

Fig. 9 POM photographs shown morphologies for PBNAd 90.9/9.1 crystallized from the melt: a) at 200°C and forming β-Crystals, b) at 200°C and then heated to the melting temperature region, c) at 205°C, d) the same as c but for longer time, e) at 205°C and f) the same as e but for longer time.

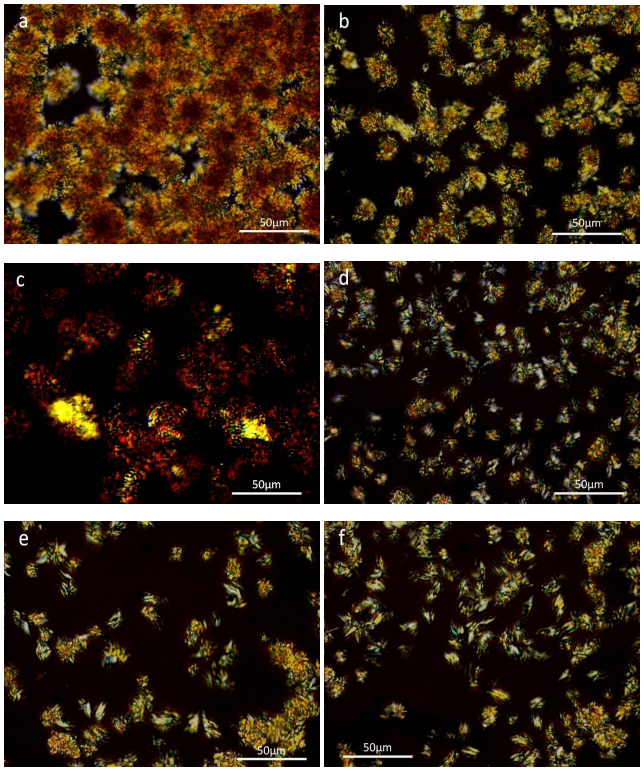

Fig. 10 PLM photographs showing the morphology of the crystallized PBN samples: a) at 220°C, α-crystals are formed, b) at 225°C, mainly α-crystals, c) at 225°C and heated to 240°C, ring-banded spherulites related to α-crystals are shown, d), e) and f) at 230°C, 232°C and 234°C respectively, with structures corresponding to β-crystals being more obvious with increasing temperature.

Thermodynamics of Melting point depression

The thermodynamics of cocrystallization in random copolymers can be analyzed on the basis of the extent of the melting point depression. In copolyesters where both components are crystallizable, a drop in the degree of crystallinity is observed as the minor component content increases if the crystal lattices of the two components are incompatible. In contrast, compatibility of the two crystallizable units in each crystal lattice can lead to cocrystallization. Allegra and Bassi reported two cases of

cocrystallization.[57] If the two components have similar chemical structure, with about the same volume, then only one crystalline phase containing both comonomer units appears at all compositions. In this case, called Isomorphism, a clear melting temperature or some crystallinity is observed over the entire copolymer composition. In contrast, if formation of two crystalline phases occurs combined with the appearance of a minimum in the plot of the melting point and the crystallinity with composition resulting in pseudo-eutectic behavior, then cocrystallization is characterized as isodimorphism.[57]

Several theories have been introduced for the copolymer crystallization. There is distinction between those which assume comonomer exclusion and those which assume comonomer inclusion in the crystal. Representative of the class of theories for comonomer exclusion are those of Flory[58-59] or Baur.[60] The most known theories of comonomer inclusion are those of Inoue,[61] Helfand-Lauritzen[62] and Sanchez-Eby.[63]

In the equation of Flory:[59]

$$\frac{1}{T_m^o} - \frac{1}{T_m(X_B)} = \frac{R}{\Delta H_m^o} \ln(1 - X_B) \qquad (4)$$

X_B is the concentration of the minor comonomer B units in the polymer and $\ln(1 - X_B)$ equals the collective activities of A sequences in the limit of the upper bound of the melting temperature. T_m^o and ΔH_m^o are the homopolymer equilibrium melting temperature and heat of fusion and R is the gas constant.

The Sanchez-Eby is based on the assumption that B comonomer units are included into the crystals of A forming defects. The corresponding equation is: [63]

$$\frac{1}{T_m^o} - \frac{1}{T_m(X_B)} = \frac{R}{\Delta H_m^o} \ln(1 - X_B + X_B e^{-\epsilon / RT}) \qquad (5)$$

where, $X_B e^{-\epsilon / RT}$ is the equilibrium fraction of repeat units B that are able to crystallize, and ϵ is the excess free energy of a defect created by the incorporation of one B unit into the crystal.

In the theory of Baur, homopolymer sequences of length ξ may be included into crystals of lamellar thickness corresponding to that length:[60]

$$\frac{1}{T_m^o} - \frac{1}{T_m(X_B)} = \frac{R}{\Delta H_m^o}[\ln(1-X_B) - \langle\xi\rangle^{-1}] \quad (6)$$

where $$\langle\xi\rangle = [2X_B(1-X_B)]^{-1} \quad (7)$$

is the average length of homopolymer sequences in the melt.

Combining both inclusion and exclusion models, the model of Wendling-Suter, is given by:[64-66]

$$\frac{1}{T_m^o} - \frac{1}{T_m(X_B)} = \frac{R}{\Delta H_m^o}\left[\frac{\in X_{CB}}{RT} + (1-X_{CB})\ln\frac{1-X_{CB}}{1-X_B} + X_{CB}\ln\frac{X_{CB}}{X_B} + \langle\tilde{\xi}\rangle^{-1}\right] \quad (8)$$

where X_{CB} is the concentration of the B units in the crystal. In the equilibrium comonomer inclusion, the concentration of B units in the crystal is given by:

$$X_{CB}^{eq} = \frac{X_B e^{-\in/RT}}{1-X_B+X_B e^{-\in/RT}} \quad (9)$$

Substitution of X_{CB} in equation 8 by equation 9, gives a simplified equation following equilibrium inclusion model:

$$\frac{1}{T_m^o} - \frac{1}{T_m(X_B)} = \frac{R}{\Delta H_m^o}\{\ln(1-X_B+X_B e^{-\in/RT}) - \langle\tilde{\xi}\rangle^{-1}\} \quad (10)$$

where

$$\langle\tilde{\xi}\rangle^{-1} = 2(X_B - X_B e^{-\in/RT})\cdot(1-X_B+X_B e^{-\in/RT}) \quad (11)$$

The limiting case of uniform inclusion is reached if $X_{CB} = X_B$ while for $X_{CB} = 0$ equation 8 is reduced to the exclusion model.

In this work the above thermodynamic models were tested. The temperature corresponding to the end of the melting peak was used, as an approach of the equilibrium melting temperature. Also, in calculations, the equilibrium melting

enthalpy of PBN was taken to be 33 kJ/mol.[24] For PBAd it was assumed to be 21.46kJ/mol.[67, 68]

The excess free energy for the copolymers as a function of the composition is plotted in Fig. 11a. As can be seen exclusion of the comonomer butylene adipate units from the PBN crystal should be rather preferred. The experimental melting points and the theoretical values calculated using the Flory, Baur, Sanchez-Eby and Wendling-Suter equations are shown in Fig. 11b. The Baur's prediction seems to be realistic. This verifies that the quite different sizes of the two comonomers do not favor of comonomer inclusion.

Among the models tested in this work the most satisfactory fit to the experimental data in the range of low comonomer content was achieved using the Wendling-Suter model. The value of the function ϵ/RT is determined as an adjustable parameter. A constant ϵ/RT value is given by the model regardless of the comonomer composition. In case of PBN best fit to the experimental data was observed assuming a value ϵ/RT=2.3. Then, calculation of the average defect free energy in the case of incorporation of BAd unit into the PBN crystal, for PBN ($X_{BAd} = 0$), resulted in ϵ = 10.3 kJ/mol. This value is quite large, showing the creation of a defect in the PBN crystal.

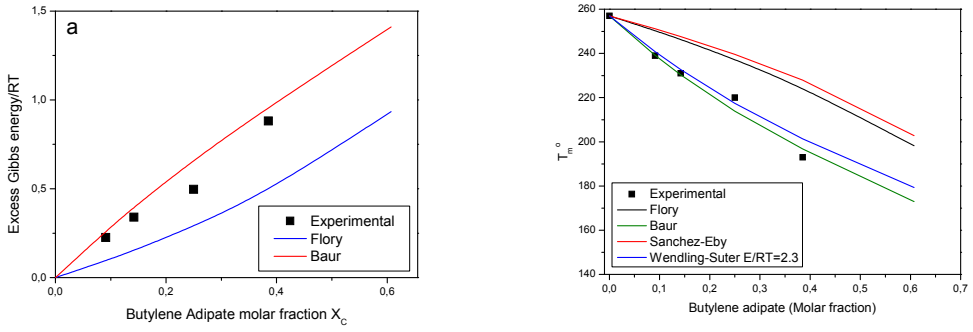

Fig. 11 a) Excess free energy and b) experimental and predicted melting point as a function of the butylene adipate content.

Results of the analysis of ^{1}HNMR spectra shown in Table 1 verify that PBN crystals are formed when the butylene naphthalate block length is bigger than that of the butylene adipate. The PBNAd 37.5/62.5 copolymer was the last having this characteristic despite the fact that butylene naphthalate was the minor comonomer. This evidences the importance of the block length for copolymer crystallization.

The case of copolymers forming PBAd crystal was also of importance. In the plots of the excess Gibbs energy one can that experimental values are very high Fig. 12a. Also, in the plots of the melting points it can be seen that neither the Flory nor the Baur model can predict the behavior of the copolymers Fig. 12b. In the Wendling-Suter a very large ϵ/RT value 4 is needed to approximate the experimental values and this results in ϵ=11.65 kJ/mol.

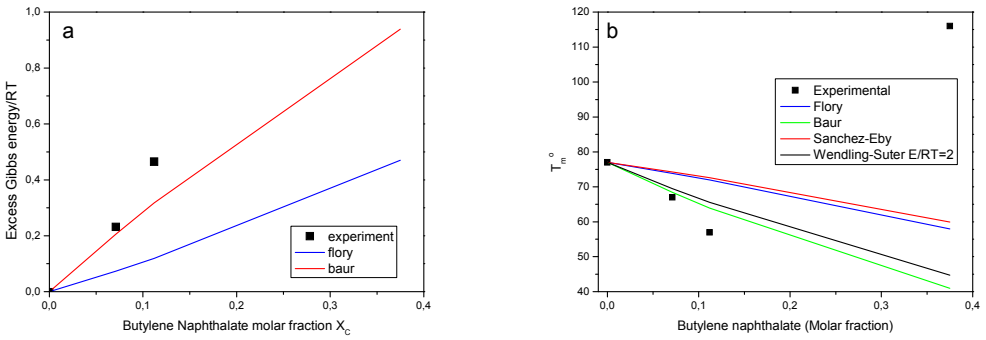

Figure 12. a) Excess free energy, b) experimental and predicted melting point as a function of the butylene naphthalate content.

The minor comonomer units amounts which were incorporated in the crystals were calculated using the results from the Wendling-Suter model. Using equation 9 the equilibrium concentrations X_{CBAd} of comonomer units in the PBN crystals were calculated and they are plotted as a function of the concentration of BAd units in the copolymer (X_{BAd}) in Fig. 13a. As it can be seen X_{CBAd} is much lower than the copolymer concentration in the bulk. The plot of X_{CBAd} versus X_{Bad} shows curvature and it has an increasing slope. The physical meaning is that in an already imperfect crystal lattice it is easier to create the excess volume necessary for a comonomer unit [26]. Furthermore, the plot of the equilibrium concentration X_{CBN} of BN units in the PBAd crystal is also shown in Fig. 13a. In this case the values of X_{CBN} are even lower than those of X_{CBAd}. This shows that it is much more difficult BN units to be included in the PBAd crystal.

In Fig. 13b one can see the dependence of the butylene naphthalate block length and also the butylene naphthalate molar fraction in the crystal as a function of the concentration of the minor comonomer butylene adipate in the bulk. The trends

are very similar, showing that there is a direct correlation between the block length and the monomer concentration in the crystal.

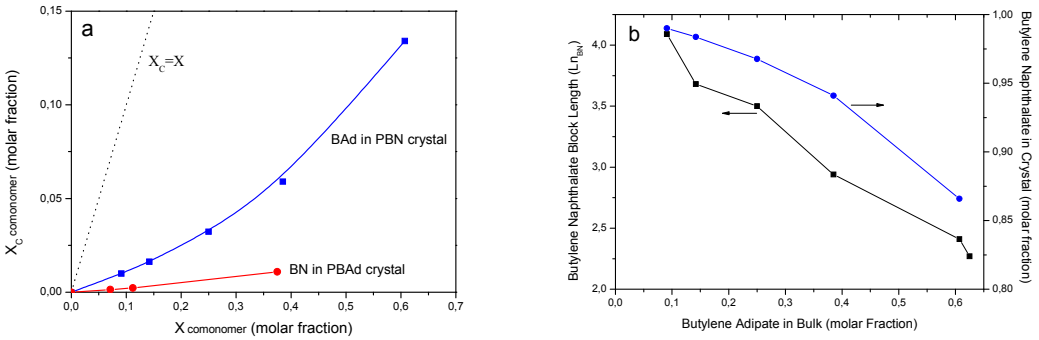

Fig. 13 a) Molar fraction of the minor comonomer in the crystal of the major comonomer vs the concentration in the bulk and b) butylene naphthalate block length and butylene naphthalate molar fraction in crystal vs the concentration of butylene adipate in the bulk.

It is finally important that the glass transition temperatures for the as received samples, which were significantly crystallized, were found to be lower than those for the amorphous. This fact was also observed in other random copolymer systems like poly(butylene-co-propylene succinate), pol(propylene terephthalate-co-succinate)s and poly(propylene terephthalate-co-adipate)s. The phenomenon should be attributed to the some segregation of crystallizable and noncrystallizable chain segments during the crystallization. In most cases, butylene adipate units are excluded from the crystals and thus, crystallization results in enrichment of the amorphous phase in flexible butylene adipate segments.

Enzymatic Hydrolysis Study

As it is known, the enzymatic degradation rates of polyesters depend on various factors, as the degree of crystallinity, the chemical structure, the melting point and the molecular mobility of the amorphous phase.[46] The study of enzymatic hydrolysis of PBAd, PBNAd 7.1/92.9, PBNAd 11.2/88.8, PBNAd 37.5/62.5 w/w, PBNAd 39.3/60.7 w/w and PBNAd 61.5/38.5 was carried out using *Pseudomonas Ceracia* and *Rhizopus delemar* lipases at 37°C. The plots of mass loss per unit surface as a function of time are presented in Fig. 14.

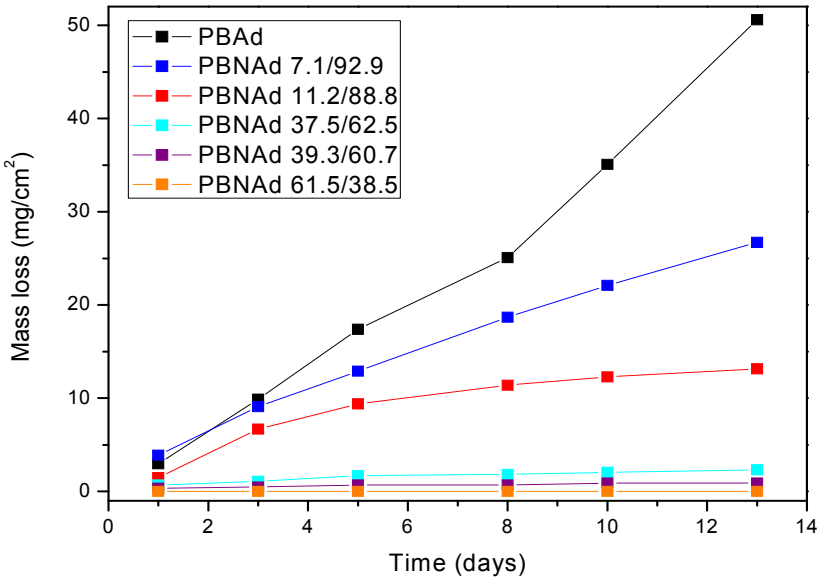

Fig. 14. Weight loss against the time of hydrolysis of the PBAdN copolymers.

As was expected, the enzymatic hydrolysis rates of the studied copolymers decreased with increasing the naphthalate content, because the attack onto the ester groups by the enzymes is sterically hindered. Naphthalate units are bulkier than adipates and thus enzymes cannot access these ester groups to hydrolyze them. This is very common in aliphatic/aromatic copolyesters.[45, 47] As a result, the PBAd showed the largest mass loss. The copolymers with 37.5% and 39.3% w/w naphthalate content showed low mass loss. Finally, PBNAd 61.5 did not hydrolyze. Naphthalate dyads or longer sequences are the non-hydrolyzable segments of the copolymers. The block length of naphthalate sequences increased with increasing the naphthalate content of copolymers and becomes significant. The melting point also increased with naphthalate content, while the amorphous fraction and the mobility of the amorphous phase decreased. Furthermore, biodegradation rates were reduced along the time because of the fact that the crystallinity of the sample increased since the amorphous phase of the polymer is hydrolyzed much faster than the crystalline phase. This was also revealed from SEM micrographs of the studied samples during enzymatic hydrolysis. As can be seen in Fig. 15 unaffected spheroulites are clearly found in all samples after the first days of hydrolysis. Furthermore, the surface of the samples with high naphthalate content, PBNAd 39.3/60.7 and PBNAd 61.5/38.5 is less eroded, which is in well agreement with mass loss of the particular samples.

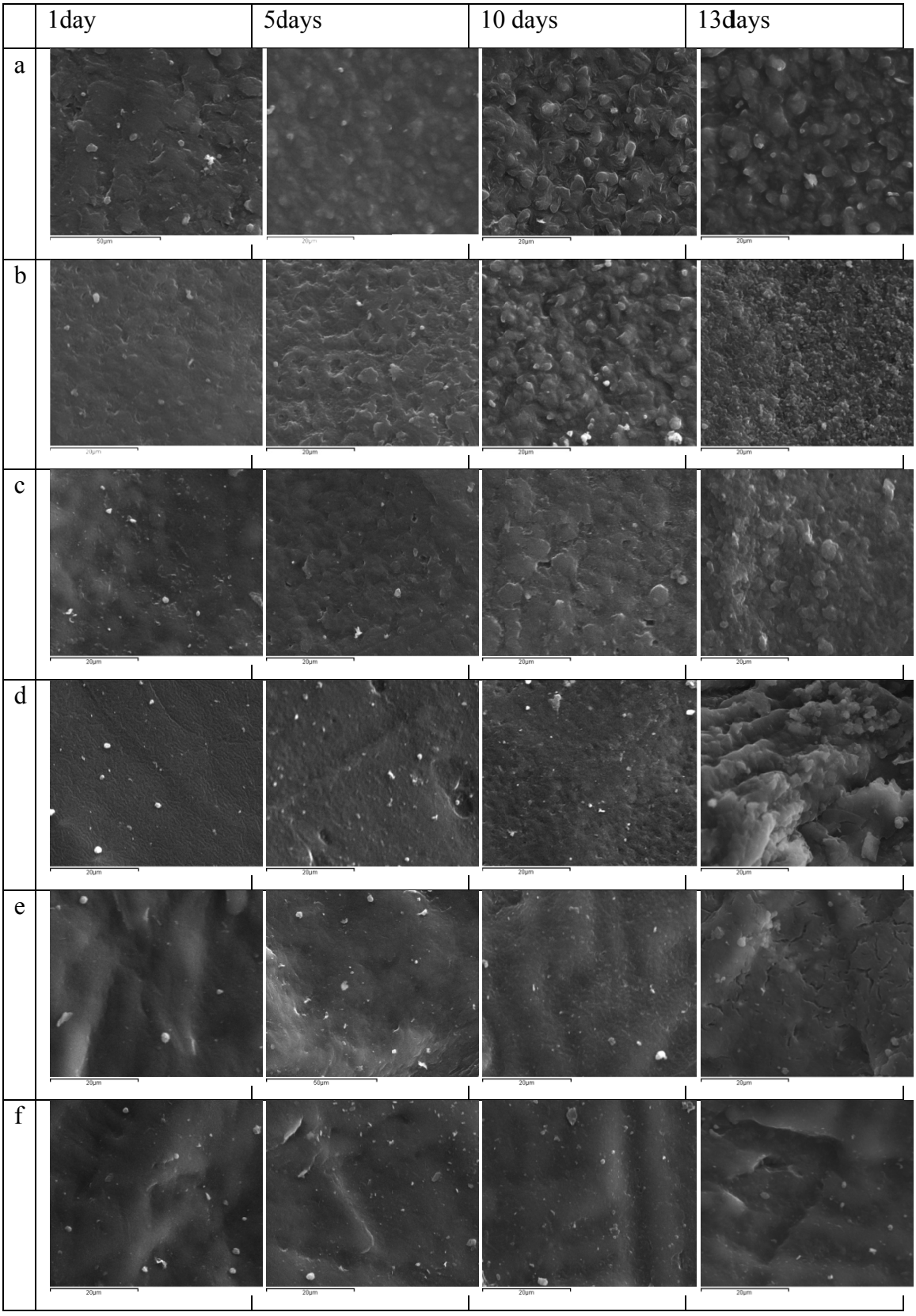

Fig. 15 SEM images showing the resulting morphology on the surface of specimens of PBAd and the PBNAd copolymers at different times of enzymatic hydrolysis: a)

PBAd, b) PBNAd 7.1/92.9, c) PBNAd 11.2/88.8, d) PBNAd 37.5/62.5, e) PBNAd 39.3/60.7 and f) PBNAd 61.5/38.5.

Conclusions

PBNAd copolyesters showed isodimorphic cocrystallization. In copolymers with low butylene adipate content β-PBN crystals were formed, thus copolymerization proved to be a tool for controlling polymorphism of PBN. Intriguing dendritic superstructures based on β-PBN crystals were observed for low adipate content. Isodimorphic cocrystallization was proved by the minimum in the plot of the melting point against composition and the fact that the copolymers with high Butylene Naphthalate units content form PBN-like crystals, while those with very high Butylene Adipate units content give PBAd-like crystals. The composition where the change from the one to the other type of crystals is observed, is that corresponding to the minimum in the melting point. Cocrystallization imposed variations in the unit cell dimensions evidenced by the changes in the interplanar spacings. For up to 40mol% butylene naphthalate content the copolymers showed significant mass loss during enzymatic hydrolysis. This fact was also supported by the changes in the appearance of the corresponding specimens evidenced by the SEM microphotographs.

References

1 K. Bechtold, M.A. Hillmyer, W.B. Tolman, *Macromolecules,* 2001, **34,** 8641-8648.

2 U. Witt, R. J. Muller, W. D. Deckwer, *Macromol. Chem. Phys.,* 1996, **197,** 1525–1535.

3 Y. Tokiwa, T. Ando, T. Suzuki, T. Takeda, *Polym. Mater. Sci. Eng.,* 1990, **62,** 988-992.

4 Y. Maeda, T. Maeda, K. Yamaguchi, S. Kubota, A. Nakayama, N. Kawasaki, N. Yamamoto, S. Aiba, *J. Polym. Sci. Part A: Polym. Chem.,* 2000, **38,** 4478-4479.

5 G. Z. Papageorgiou, S. G. Nanaki, D. N. Bikiaris, *Polym. Degrad. Stab.,* 2010, **95,** 627-637.

6 H. C. Ki, O. O. Park, *Polymer,* 2001, **42,** 1849–961.

7 M. Atfani, F. Brisse, *Macromolecules,* 1999, **32,** 7741–52.

8 L. Wu, R. Mincheva, Y. Xu, J. M. Raquez, P. Dubois, Biomacromolecules, 2012, **13**, 2973–2981.

9 G. Giammanco, A. Martínez De Ilarduya, A. Alla, S. Muñoz-Guerra, *Biomacromolecules,* 2010, **11,** 2512-2520.

10 W.D. Li, J.-B. Zeng, X.-J. Lou, J.-J. Zhang, Y.-Z. Wang, *Polymer Chemistry,* 2012, **3,** 1075-1083.

11 N. González-Vidal, A. Martínez De Ilarduya, V. Herrera, S. Muñoz-Guerra, *Macromolecules,* 2008, **41,** 4136-4146.

12 U. Witt, M. Yamamoto, U. Seeliger, R. J. Muller, *Warzelhan, V. Angew. Chem. Int. Ed.,* 1999, **38,** 1438–42.

13 R. J. Muller, I. Kleeberg, W. D. Deckwer, *J. Biotechnol.,* 2001, **86,** 87–95.

14 T. Kijchavengkul, R. Auras, M. Rubino, M. Ngouajio, R. T. Fernandez, *Chemosphere,* 2008, **71,** 1607–1616.

15 P. Rychter, M. Kawalec, M. Sobota, P. Kurcok, M. Kowalczuk, *Biomacromolecules,* 2010, **11,** 839-847.

16. I. Kleeberg, K. Welzel, J. VandenHeuvel, R.-J. Müller, W.-D. Deckwer, *Biomacromolecules,* 2005, **6,** 262-270.

17 M. Yamamoto, U. Witt, D. I. G. Skupin, Biopolymers, volume 4. In: Doi Y, Steinbuchel A, editors. Polyesters III: applications and commercial products. Weinheim: Germany: Wiley-VCH Verlag GmbH; 2002. p. 299.

18 Z. Gan, K. Kuwabara, M. Yamamoto, H. Abe, Y. Doi, *Polym. Degrad. Stab.,* 2004, **83**, 289–300.

19 Siegenthaler, K. O.; Künkel, A.; Skupin, G.; Yamamoto, M. *Adv. Polym. Sci.* **2012**, *245*, 91-136.

20 X. Q. Shi, H. Ito, T. Kikutani, *Polymer,* 2005, **46**, 11442–11450.

21 M. Weng, Z. Qiu, *Thermochimica Acta,* 2014, **575,** 262– 268.

22 M.Okada, *Prog. Polym. Sci,.* 2002, **27**, 87–133.

23 M. Renke-Gluszko, M. El Fray, *Biomaterials,* 2004, **25,** 5191–5198.

24 Y. G. Jeong, W. H. Jo, S. C. Lee, *Macromolecules,* 2000, **33,** 9705-9711.

25 G. P. Karayannidis, G. Z. Papageorgiou, D. N. Bikiaris, E. V. Tourasanidis, *Polymer,* 1998, **39,** 4129-4134.

26 Y. G. Jeong, W. H. Jo, S. C. Lee, *Macromolecules,* 2003, **36,** 4051-4059.

27 G. Z. Papageorgiou, G. P. Karayannidis, *Polymer,* 1999, **40,** 5325–5332.

28 G. Z. Papageorgiou, D. S . Achilias, G. P. Karayannidis, *Polymer,* 2010, **51***,* 2565-2575.

29 G. Z. Papageorgiou, G. P. Karayannidis, *Polymer,* 2001, **42,** 2637–2645.

30 M. Soccio, M, Gazzano, N. Lotti, L. Finelli, A. Munari, *Polymer,* 2010, **51***,* 192–200.

31 T. Zorba, K. Chrissafis, K. M. Paraskevopoulos, D. N. Bikiaris, *Polym. Degrad. Stab.* **2007**, *92*, 222-230.

32 J. Yang, P. Pan, L. Hua, B. Zhu, T. Dong, Y. Inoue, *Macromolecules,* 2010, **43**, 8610–8618.

33 Z. Liang, P. Pan, B. Zhu, Y. Inoue, *Macromolecules,* 2010, **43**, 6429–6437.

34 P. Pan, Y. Inoue, *Prog. Polym. Sci.,* 2009, **34**, 605–640.

35 J. Yang, P. Pan, L. Hua, Y. Xie, T. Dong, B. Zhu, Y. Inoue, X. Feng, *Polymer,* 2011*,* **52** 3460-3468.

36 H. Wang, Z. Gan, J. M. Schult, S. Yan, *Polymer,* 2008, **49,** 2342–2353.

37 E. Pouget, A. Almontassir, M. T. Casas, J. Puiggali, *Macromolecules,* 2003, **36**, 698-705.

38 E. M. Woo, M. C. Wu, *J. Polym. Sci.: Polym. Phys*., 2005, **43**, 1662–1672.

39 J. Liu, H. M. Ye, J. Xu, B. H. Guo, *Polymer,* 2011, **52**, 4619-4630.

40 L. Y. Wang, G. Lugito, E. M. Woo, Y. H. Wang, *Polymer,* 2012, **53,** 3815-3826.

41 Z. Gan, K. Kuwabara, H. Abe, T. Iwata, Y. Doi, *Polym. Degrad. Stab*., 2005, **87**, 191-199.

42 P. Rychter, M. Kawalec, M. Sobota, P. Kurcok, M. Kowalczuk, *Biomacromolecules,* 2010, **11**, 839–847.

43 Z. Liang, P. Pan, B. Zhu, J. Yang, Y. Inoue, *Polymer,* 2011, **52***,* 5204-5211.

44 L. Zhao, Z. Gan, *Polym. Degrad.Stab.,* 2006, **91***,* 2429-2436.

45 G. Z. Papageorgiou, D. N. Bikiaris, *Biomacromolecules,* 2007, **8,** 2437-2449.

46 D. N. Bikiaris, G. Z. Papageorgiou, D. J. Giliopoulos, C. A. Stergiou, *Macromol. Biosci.,* 2008, **8**, 728–740.

47 G. Z. Papageorgiou, A. A. Vassiliou, V. D. Karavelidis, A. Koumbis, D. N. Bikiaris, *Macromolecules,* 2008, **41,** 1675-1684.

48 B. Fillon, J. C. B. Wittmann, Lotz, A. J. Thierry, *Polym, Sci.: Polym. Phys.,*1993, **31,** 1383-1393.

49 A. J. Müller, J. Albuerne, L. Marquez, J.-M. Raquez, P. Degée, P. Dubois, J. Hobbs, I. W. Hamley, *Faraday Discuss.,* 2005, **128**, 231-252.

50 A. Boschetti-de-Fierro, A. T. Lorenzo, A. J. Müller, H. Schmalz, V. Abetz, *Macromol. Chem. Phys*., 2008, **209***,* 476-487.

51 M. Soccio, L. Finelli, N. Lotti, M. Gazzano, A. Munari, *J. Polym. Sci.: Polym. Phys.* 2007, **45**, 310-321.

52 M. Soccio, L. Finelli, N. Lotti, M. Gazzano, A. J. Munari, *Polym. Sci.: Polym. Phys.,* 2007, **45**, 310-321.

53 R. Yamadera, M. Murano, *J. Polym. Sci*.: *Polym. Chem.,* 1967, **5**, 2259–2268.

54 G. Z. Papageorgiou, D. N. Bikiaris, *Macromol. Chem. Phys.,* 2009, **210**, 1408–1421.

55 C. S. Fuller, *J. Am. Chem. Soc.,* 1937, **59**, 344–51.

56 R. Minke, J. Blackwell, *J. Macromol. Sci.-Phys.,* 1979, **B16**, 407-417.

57 G. Allegra, I. W. Bassi, Adv. Polym. Sci., 1969, **6,** 549–74.

58 P. J. Flory, *J. Chem. Phys*., 1949, **17***,* 223-226.

59 P. J. Flory, Trans. Faraday Soc., 1955, **51**, 848-857.

60 H. Baur, *Die Makromolekulare Chemie,* 1966, **98,** 297–301.

61 N. Kamiya, M. Sakurai, Y. Inoue, R. Chujo, *Macromolecules*, 1991, **24**, 3888–3892.

62 E. Helfand, J. I. Jr. Lauritzen, *Macromoelcules,* 1973, **6**, 631–638.

63 I. C. Sanchez, R. K. Eby, *Macromoelcules,* 1975, **8**, 638–641.

64. J. Wendling, A. A. Gusev, U. W. Suter, A. Braam, L. Leemans, R. J. Meier, J. Aerts, J. Van der Heuvel, M. Hottenhuis, *Macromolecules,* 1999, **32,** 7866-7878.

65. J. Wendling, A. A. Gusev, U. W. Suter, *Macromolecules*, 1998, **31**, 2509–2515.

66. J. Wendling, U. W. Suter, *Macromolecules*, 1998, **31,** 2516–2520.

67. J. P. Penning, R. St. J. Manley, *Macromolecules,* 1996, **29**, 77-83.

68. M. S. Yagforov, *Vysokomol. Soedin., Ser. A,* 1975, **17**, 2476-2479.

Graphical Abstract

Crystallization of Poly(butylene 2,6-naphthalate-co-butylene adipate)s: Regulating Crystal Modification of the Polymorphic Parent Homopolymers and Biodegradation

George Z. Papageorgiou, Vasilios Tsanaktsis, Dimitrios N. Bikiaris

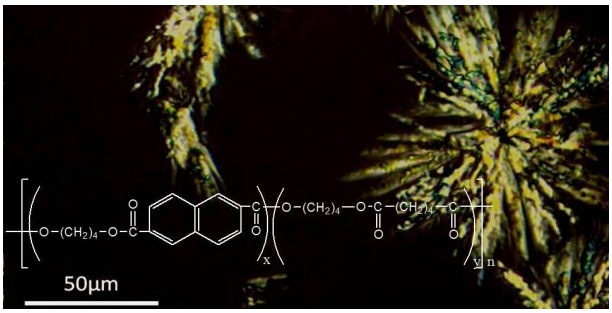

Highlights

- Random poly(butylene 2,6-naphthalate-co-butylene adipate)s were synthesized by melt polycondensation.
- The PBNAd copolymers showed isodimorphic cocrystallization.
- β-crystals of poly(butylene 2,6-naphthalate) (PBN) and large dendrites were in principle formed in copolymers with high BN content.
- The thermodynamic analysis of cocrystallization verified limited incorporation of the minor comonomer in the crystals.
- PBNAd copolymers with less than 50 mol% butylene naphthalate content exhibited significant biodegradation rates.